Theoretical and experimental investigation of the electron spin resonance of Co^{2+} in $Zn_2(OH)PO_4$ and $Mg_2(OH)AsO_4$

2002 J. Phys.: Condens. Matter 14 2025

(http://iopscience.iop.org/0953-8984/14/8/329)

INSTITUTE OF PHYSICS PUBLISHING JOURNAL OF PHYSICS: CONDENSED MATTER

J. Phys.: Condens. Matter **14** (2002) 2025–2041 PII: S0953-8984(02)30135-8

Theoretical and experimental investigation of the electron spin resonance of Co^{2+} in $Zn_2(OH)PO_4$ and $Mg_2(OH)AsO_4$

M E Foglio[1], M C dos Santos[1], G E Barberis[1], J M Rojo[2], J L Mesa[2], L Lezama[2] and T Rojo[2]

[1] Instituto de Física 'Gleb Wataghin', UNICAMP, 13083-970, Campions, São Paulo, Brazil
[2] Departamento de Química Inorgánica, Universidad del País, Vasco 48080 Bilbao, Spain

Received 26 October 2001, in final form 14 January 2002
Published 15 February 2002
Online at stacks.iop.org/JPhysCM/14/2025

Abstract

Electron spin-resonance experiments were performed on Co^{2+} substituting for Zn^{2+} or Mg^{2+} in powder samples of $Zn_2(OH)PO_4$ and $Mg_2(OH)AsO_4$. These two compounds are iso-structural and contain the Co^{2+} in two environments with approximately octahedral and trigonal bipyramidal structures. The observed resonances are described using a theoretical model that considers the departures from the two perfect structures. It is shown that resonance in the penta-coordinated complex is allowed, and the crystal fields that would reproduce the resonance of the Co^{2+} in the two environments are calculated. The low intensity of the resonance in the penta-coordinated complex is explained by assuming that this site is much less populated than the octahedral one; this assumption was verified by a molecular calculation of the energies of the two environments, with both Co and Zn as central ions in $Zn_2(OH)PO_4$.

1. Introduction

Mineral solid-state chemistry offers an important contribution to materials science [1] in the search for systems with new and useful physical properties. The phosphate and arsenate minerals crystallize in various structures, sometimes containing several non-equivalent sites for the metals. The minerals of the olivine group, with the formula $ABXO_4$, have been known for a long time [2], and the adamite family, with formula $[M_2(O/OH)(XO_4)]$, belongs to this group and takes its name from the natural compound [3, 4] $Zn_2(OH)AsO_4$. The compounds studied in this work belong to this family, and the cations can occupy two sites with rather different environments, one being octahedral and the other penta-coordinated, so rather different magnetic properties can be expected when magnetic cations are employed. The recently synthesized compounds $Zn_2(OH)PO_4$ [5], $Co_2(OH)PO_4$ [5], $Mg_2(OH)AsO_4$ [6, 7], as well as the natural $Co_2(OH)AsO_4$ [1], are of the adamite type and present these two types of site. We thus found it interesting to study the properties of the Co^{2+} ions as impurities in the

two non-magnetic compounds, as a first step in gaining an understanding of the properties of the concentrated compounds.

The electron spin-resonance (ESR) technique is fruitful as regards obtaining local information on the environment of the magnetic ion, and the Co^{2+} ion is particularly useful for this kind of study because its g-value has a strong crystal-field dependence in these compounds. To analyse the ESR measurements it is necessary to have information about the splitting of the energy levels with both the crystal field and the electronic Coulomb repulsion, and to obtain this information we employed optical diffuse reflectance measurements [8].

The experimental ESR powder spectra for Co^{2+} impurities in $Zn_2(OH)PO_4$ and $Mg_2(OH)AsO_4$ both present two different sets of lines, one very intense, and the other just observable. The average of the g-factors of the intense spectra is 4.15 in the two compounds, a value close to the 4.33 expected for Co^{2+} in moderately distorted octahedral symmetry [9], and it seems reasonable to assign these spectra to that environment and apply the approach already employed [10] in the study of the ESR of Co^{2+} in $NH_4NiPO_4{\cdot}6H_2O$, where the crystal fields that reproduce the observed spectra were obtained. As the remaining lines are very weak, one should analyse whether they belong to the penta-coordinated symmetry, and in that case the possible reasons for their low intensity.

We are not aware of any theory describing the ESR of Co^{2+} in the penta-coordinated environment, a distorted trigonal bipyramid, and we first calculated the crystal fields of the perfect trigonal bipyramid following the existing literature [11, 12]. To analyse the distorted complex we derived the normal modes of the trigonal bipyramid with respect to the reference complex, and then obtained the Jahn–Teller contributions [13, 14] to the crystal field acting on the Co^{2+}, that is generated by these modes.

In this calculation we have introduced a procedure that uniquely defines the orientation and size of the two reference complexes, so that the normal modes that describe their deformation are free from irrelevant rotations and expansions.

These results were then employed to calculate the theoretical ESR spectra [15]. We found that for the system parameters obtained from the optical spectra we should expect the ground doublet to be $M_J = \pm 1/2$, corresponding to an allowed spectrum. The rather low intensity of this type of spectrum seems to indicate a preference of Co^{2+} for the octahedral sites in the crystal structure—a conjecture that was advanced in a preliminary report [16] on the ESR of impurities of this ion in $Mg_2(OH)AsO_4$, and that is confirmed in the present work. Employing a molecular calculation we have also verified that the formation energies of the two types of complex, with Co and with Zn as the central ions, are compatible with this hypothesis.

The description of the experiments and experimental analysis of the data are presented in section 2. The theory of the ESR of the Co^{2+} in a distorted trigonal bipyramid is presented in section 3, together with the theoretical analysis of the two types of complex in the two compounds. A discussion of our results is presented in section 4 together with our conclusions.

2. Experimental procedure

2.1. Synthesis and characterization of the materials

Compounds with Co^{2+} substituting Mg and Zn in $Zn_2(OH)PO_4$ and $Mg_2(OH)AsO_4$ were prepared by hydrothermal synthesis, starting from the $(M, Co)_3(XO_4){:}8H_2O$ (M = Zn, Mg) vivianites, previously prepared as reported elsewhere [17]. Approximately 0.200 g of these precursors were disaggregated in about 75 ml of water and were placed in a poly(tetrafluoroethylene)-lined stainless steel container (about three-quarters full) under autogenous pressure. The reaction was carried out at 180 °C and maintained for one week. The resulting microcrystalline products were filtered off and washed with ether and dried in air.

Table 1. (a) The transitions between the ground $^4T_{1g}$ level and the levels shown at the top of each column, in cm^{-1}, and assigned from the experimental spectra of the octahedral complexes of $Co_2(OH)PO_4$ and $Co_2(OH)AsO_4$; the level $^4T_{1g}(P)$ corresponds to the highest one of the same symmetry. (b) The best fit, obtained with the values of B and Dq shown in the last two columns.

$^4T_{1g} \rightarrow$	$^4T_{2g}$	$^4A_{2g}$	$^4T_{1g}(P)$	B	Dq
PO_4					
(a)	8450	15 450	18 350		
(b)	7819	16 013	18 324	767.6	819.4
AsO_4					
(a)	7700	15 500	18 020		
(b)	7616	15 585	18 011	758.9	796.9

The results of the analysis of Mg, Zn, Co, P, and As by inductively coupled plasma atomic emission spectroscopy (ICPAES) are in good agreement with the proposed formulae. The compounds were also characterized by x-ray powder diffraction, using the Rietveld method. The diffractograms were indexed with the $Pnnm$ space group and the lattice parameters $a = 8.042(3)$ Å, $b = 8.369(2)$ Å, and $c = 5.940(2)$ Å for the phosphate compound and $a = 8.286(2)$ Å, $b = 8.594(2)$ Å, and $c = 6.051(1)$ Å for the arsenate. The parameters of the phosphate compound are only slightly different from those given in [5], while those of the arsenate coincide with the data published by other authors [6, 7]; the results obtained in the last three references were from investigations performed on single crystals. The x-ray powder pattern was recorded employing Cu Kα radiation with a PHILIPS X'PERT automatic diffractometer, with steps of 0.02° in 2Θ and fixed-time counting of 1 s in the $5^\circ < 2\Theta < 70^\circ$ range. We preferred to use our own experimental parameters in the present paper.

2.2. Optical studies

The necessary optical data were obtained from diffuse reflectance experiments, performed in a CARY 2415 UV–VIS–IR spectrometer, controlled with a VARIAN DS15 workstation, in the 5000–50 000 cm^{-1} wavenumber region [8, 18]. The whole set of optical data used in this work was recorded at room temperature, and all the relevant data that were needed in the present work are given in tables 1 and 2. Figure 1 presents the experimental data for both the phosphate and the arsenate Co compounds studied in this paper. The system parameters of the octahedral complexes are slightly different from those already published [8, 18], because they were obtained from the optical spectra after including a spin–orbit correction in the ground orbital level[3].

2.3. Electron spin resonance (ESR)

The ESR spectra were performed at X Band on a Bruker ESP300 spectrometer. Cooling and temperature control of the samples were achieved with a standard OXFORD helium continuous-flow cryostat, included in the microwave cavity. Magnetic field measurements were made simultaneously with the ESR spectra recording, using a Bruker ER035M NMR gaussmeter. The resonant frequency of the cavity was measured with a Hewlett-Packard 5352B microwave frequency counter.

[3] When we derived the system parameters of the octahedral complexes from the optical spectra, we shifted the ground orbital level by the spin–orbit correction, estimated to be $2.5\alpha\lambda \sim -635$ cm^{-1}. This improvement was not used for the penta-coordinated complex.

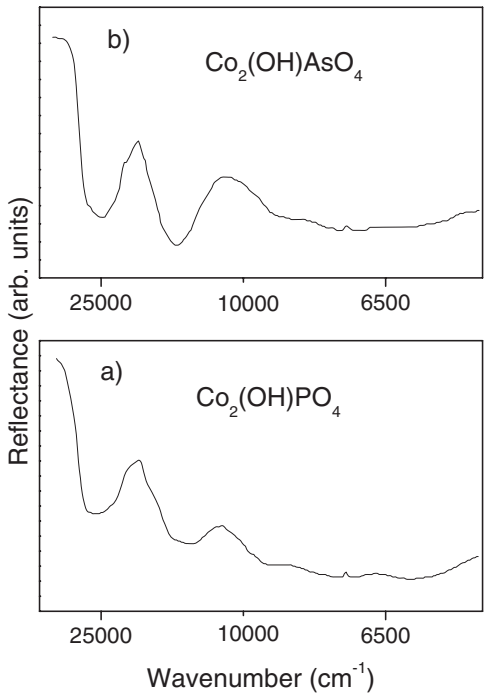

Figure 1. Diffuse reflectance spectra for (*a*) $Co_2(OH)PO_4$ and (*b*) $Co_2(OH)AsO_4$. The horizontal scale is linear in the wavelength, but has been labelled employing the corresponding wavenumbers.

Table 2. (a) The transitions between the ground level $^4A_1''$ and the levels shown at the top of each column, given in cm^{-1}, and assigned from the experimental spectra of the penta-coordinated complexes of $Co_2(OH)PO_4$ and $Co_2(OH)AsO_4$. (b) The best possible fit to the five transitions. (c) The best fit obtained by adjusting only the three transitions of higher energy. The corresponding values of B, D_s, D_t are given in rows (b) and (c) of table 5.

$^4A_2' \rightarrow$	$^4A_1'', {}^4A_2''$	$^4E''$	$^4E'$	$^4A_2'(P)$	$^4E''(P)$
PO_4					
(a)	6400	7000	11 100	15 800	19 600
(b)	3233	4835	12 868	17 386	17 947
(c)	1511	3603	11 106	15 801	19 604
AsO_4					
(a)	5000	6250	10 870	16 000	19 800
(b)	2707	4440	12 210	17 188	18 595
(c)	1437	3535	10 876	15 999	19 805

Only powder spectra could be measured for the two systems studied here because it was not possible to obtain single crystals, and small concentrations of Co (1% in the arsenate and 0.1% in the phosphate) substitute for the metals in the two lattices. The curves labelled (a) in figures 2 and 3 show the measured ESR spectra for the two samples, recorded at 4.2 K, and they both clearly show three sets of lines with a well defined hyperfine structure that identifies

Table 3. Values of the principal g- and A-parameters, obtained from the spectra in figures 2 and 3. The values of the A-parameters are in units of 10^{-4} cm^{-1}. (a) The octahedral complex: the g- and A-values were obtained from a program simulating powder spectra, as described in the text. (b) The parameters for the penta-coordinated Co^{2+}, also estimated by simulation.

	g_1	g_2	g_3	A_1	A_2	A_3
PO_4						
(a)	5.89 ± 0.02	4.55 ± 0.05	2.02 ± 0.02	240 ± 5	155 ± 8	85 ± 3
(b)	8.0 ± 0.5	3.2 ± 0.3	2.0 ± 0.2			
AsO_4						
(a)	6.22 ± 0.02	4.21 ± 0.05	2.05 ± 0.02	140 ± 5	120 ± 7	55 ± 5
(b)	9.0 ± 1.5	3.0 ± 0.5	2.0 ± 0.2			

the Co^{2+} ion. There are also some extra lines, rather weak for the phosphate but more intense for the arsenate, that preclude an automatic fitting of the spectra. We then simulated the powder spectra of the hexa-coordinated Co^{2+} with a program which allows any symmetry, line position, hyperfine tensor, and linewidth anisotropy, and our best results, plotted as curves (c) of figures 2 and 3, correspond to the g-values shown in rows (a) of table 3. Their values and positions are also shown by arrows below the simulated curves (c).

The extra lines near 200 mT for the phosphate show a hyperfine structure typical of the Co^{2+}, and are given in more detail in the inset of figure 2. The remaining lines for the two compounds are rather broad and show a collapsed hyperfine structure. Curve (b) shows the sum of the simulated spectrum of the hexa-coordinated Co^{2+} (c) and a simulation of the penta-coordinated Co^{2+} that employs the g-values given in rows (b) of table 3 and is appropriately renormalized to account for the smaller relative concentration of the latter, in figures 2 and 3. These g-values have rather large errors, and their positions are shown by arrows above the measured spectra (a) of figures 2 and 3. In the inset of figure 2 we also show the detail of the hyperfine structure near 200 mT both in the experimental and in the simulated spectrum.

The assignment of the extra lines to the penta-coordinated complex will be further discussed in section 3.5.

3. Theoretical discussion

3.1. Hexa-coordinated Co

We shall first discuss the hexa-coordinated Co^{2+} ions, that are surrounded by six oxygens in a fairly regular octahedron [15]. In the present case we have a powder spectrum, and we could only measure the three principal values g_i of the **g**-tensor (see table 3). As in a previous work [10], we shall consider the effect that the crystal field generated by the normal modes of the octahedron has on the gyromagnetic tensor **g**. This method systematizes the procedure for obtaining that field, and in table 4 we give the normal modes that reproduce the experimental values of the three g_i. We shall then choose a reference perfect octahedron centred on the Co^{2+}, calculate the normal modes corresponding to the crystallographic positions of the O, and compare them (in table 4) with those obtained from the experimental spectra.

Only the normal coordinates that are invariant under inversion with respect to the centre of the octahedron are necessary in the present problem [10, 19], and these are separated into the three sets $\{Q_1\}$, $\{Q_2, Q_3\}$, and $\{Q_4, Q_5, Q_6\}$, with the corresponding Q_j transforming respectively like the bases of the irreducible representations A_1, E, and T_2 of the cubic group, as given in table 2 of [20].

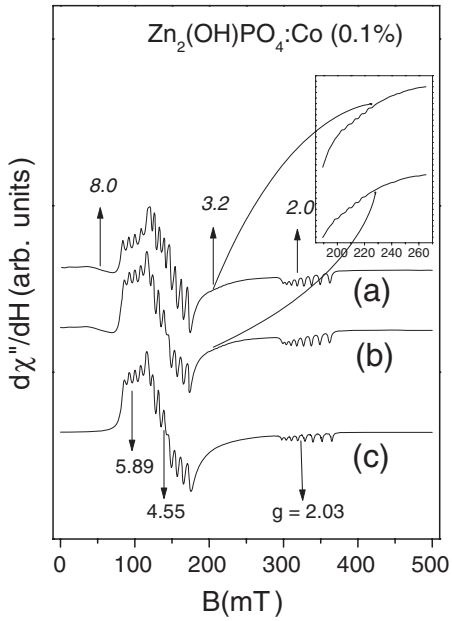

Figure 2. ESR spectra of Co^{2+} in $Zn_2(OH)PO_4$. (a) The experimental spectrum. (b) The sum of the simulated spectrum for the hexa-coordinated complex and that for the penta-coordinated complex. (c) The simulated spectrum for the hexa-coordinated complex. The g-values of the octahedral complex and the penta-coordinated complex are given in table 3. The arrows on (c) show the g-values and their positions for the octahedral complex, while those on (a) correspond to the penta-coordinated complex. The inset gives the detail of the experimental hyperfine structure and of the simulated one (around g_2), attributed to the Co^{2+} in the triangular bipyramid.

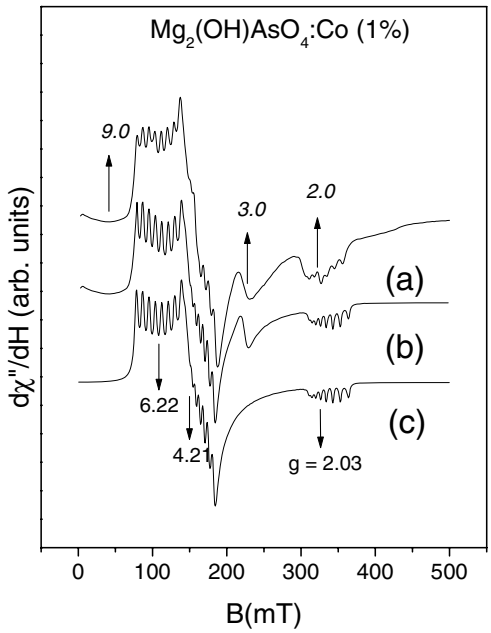

Figure 3. ESR spectra of Co^{2+} in $Mg_2(OH)AsO_4$. Curves (a), (b), and (c), and the meanings of the arrows and values on curves (a) and (c), are as for figure 2.

Table 4. Normal modes of the octahedral Co divided by the Co–O distance R in Co:$Zn_2(OH)PO_4$ and Co:$Mg_2(OH)AsO_4$. (a) Values that adjust the experimental values of the **g**-tensor. (b) Values obtained from the crystallographic positions corresponding to the pure compounds.

	Q_2/R	Q_3/R	Q_4/R	Q_5/R	Q_6/R
PO_4					
(a)	0	−0.044 07	0.034 78	0.034 78	0.114 25
(b)	0	−0.116 83	−0.017 17	−0.017 17	−0.056 41
AsO_4					
(a)	0	−0.0441	0.040 32	0.040 32	0.099 89
(b)	0	−0.093 28	−0.028 18	−0.028 18	−0.069 82

In a purely octahedral crystal field, the ^4F ground state for isolated Co^{2+} ($3d^7$) splits into two orbital triplets, $^4T_1$, $^4T_2$, and one orbital singlet, $^4A_2$. Spin–orbit effects partially lift the degeneracy of the $^4T_1$ triplet into one Γ_6, one Γ_7, and two Γ_8 subspaces, and the resonance for the lowest doublet (Γ_6) is isotropic with $g = 4.33$ [9]. The addition of lower-symmetry crystal fields produces further splitting of the $^4T_1$ triplet, giving six Kramers doublets, and in most cases it is found that the trace of the **g**-tensor is close to the cubic isotropic value [21]; in the present case the average value of g is 4.1537 for Co:$Zn_2(OH)PO_4$ and 4.153 for Co:$Mg_2(OH)AsO_4$. To understand these values it is sufficient to consider the Co^{2+} in pure octahedral symmetry; the analysis of this result follows closely that employed in [10] and will not be repeated here [15].

In the lowest order one obtains **g** from the matrix elements of the Zeeman term in the Γ_6 subspace of the $^4T_1$ ground triplet. The matrix elements of the orbital angular momentum $\boldsymbol{L}$ within the lowest T_1 subspace are proportional to those of a P term, and the proportionality constant $\alpha = -1.4110$ is affected by the mixing with the excited term ^4P, that is also of $^4T_1$ symmetry. Its value can be obtained [15] from the Racah parameter B and the crystal-field parameter Dq, that were estimated from the spectroscopic data and are given in table 1.

To analyse further the experimental **g**-tensor, one could try to find crystal-field values that would reproduce the measured results, and a study of this type was presented by Abragam and Pryce for the cobalt Tutton salts [22]. To simplify the study, we present a model that describes all the crystal fields acting on the Co as originating in the crystal field of the six nearest O located at the vertices of a deformed octahedron, obtained by displacement of the vertices of the reference octahedron. If one neglects the mixing of other configurations into the ground configuration $(3d)^7$, it is sufficient to keep only the part of the crystal field V that is even under inversion. We can then write $V = \sum_{i=1}^{7} V(\boldsymbol{r}_i)$, where $V(\boldsymbol{r})$ is the sum of homogeneous polynomials of second and fourth order in the components x, y, z of the electronic coordinates $\boldsymbol{r}$. Within our model, one could then write [19]

$$V(\boldsymbol{r}) = \sum_j Q_j V_j(\boldsymbol{r}) \tag{1}$$

where the Q_j and $V_j(\boldsymbol{r})$ transform like the same partners of irreducible representations of the octahedral group [20]. As the$V_j(\boldsymbol{r})$ must be even under inversion, the Q_j must have the same property, an only the six Q_j with $j = 1, \ldots, 6$ discussed at the beginning of this section would appear in equation (1), but we shall not consider the identical representation A_1 because it does not modify the **g**-tensor. The useful $V_j(\boldsymbol{r})$ are given in equations (4)–(6) from [10].

To study the effect that $V(\boldsymbol{r})$ given in equation (1) has on the **g**-tensor of, we shall employ second-order perturbation theory [23], using both $V(\boldsymbol{r})$ and the Zeeman term $H_Z = (g_e\boldsymbol{S} + \boldsymbol{L}) \cdot \boldsymbol{H}$ as perturbations. The change $\delta\mathbf{g}$ in the **g**-tensor is then obtained from

$$\boldsymbol{S}\,\delta\mathbf{g}\,\boldsymbol{H} = \frac{2}{3}(g_e+\alpha)\frac{\mu_B}{\Delta}\{-C_E[\sqrt{3}Q_2(S_xH_x - S_yH_y) + Q_3(3S_zH_z - \boldsymbol{S}\cdot\boldsymbol{H})] + C_T[Q_4(S_zH_y + S_yH_z) + Q_5(S_xH_z + S_zH_x) + Q_6(S_xH_y + S_yH_x)]\}, \quad (2)$$

where μ_B is the Bohr magneton, Δ is the splitting between the Γ_6 doublet and the lowest Γ_8 quadruplet in the octahedral symmetry, and $\Delta = 283\ \mathrm{cm}^{-1}$ in the P compound.

The values $C_E = 6436\ \mathrm{cm}^{-1}\ \mathrm{Å}^{-1}$ and $C_T = -3666\ \mathrm{cm}^{-1}\ \mathrm{Å}$ were obtained employing the Co–O distance [15] $R = 2.111\,76\ \mathrm{Å}^{-1}$. We can now calculate the crystal fields that would reproduce the experimental values of **g** or, equivalently, the corresponding normal modes within the approximations just discussed. As there are more normal modes than data, we fix the relations $Q_4 = Q_3 = 0.3044Q_6$, which correspond to the normal modes calculated below from the crystallographic positions, and we obtain a perfect fit to the experimental values employing the normal modes given in table 4.

For $Co_2(OH)AsO_4$ one obtains $\alpha = -1.4128$, $\Delta = 282\ \mathrm{cm}^{-1}$, and $R = 2.1224$ Å, so $C_E = 6287\ \mathrm{cm}^{-1}\ \mathrm{Å}^{-1}$, and $C_T = -3558\ \mathrm{cm}^{-1}\ \mathrm{Å}^{-1}$. As before, we fixed $Q_4 = Q_3 = 0.4037Q_6$.

To calculate the crystallographic normal modes of the octahedron it is necessary to choose a reference perfect octahedron centred on the Co^{2+}. To this end, we consider the three normal modes of pure rotation [19], Q_{19}, Q_{20}, and Q_{21}, and we choose the axes of the reference octahedron such that these three normal coordinates are zero, because they should not have any effect on the properties of the complex. The value $R = 2.111\,76$ Å of the Co–O distance in the reference octahedron was chosen so that $Q_1 = 0$, and by this procedure we obtain a unique reference octahedron and minimize the effect of irrelevant rotations and expansions on the values of the normal modes. With the crystallographic ionic positions with respect to this reference octahedron, we found the normal modes given in the third line of table 4. This normal modes are different from those given in the first line of the same table, that were obtained from the experimental **g**-tensor. This result indicates that although the nearest O to the Co are the main source of the cubic field [19], the remaining non-cubic perturbations contain strong contributions due to the rest of the crystal. We conclude that the experimental **g**-tensor could be explained by the crystal field $V(r)$ of equation (1), given in relation to the axes of the reference octahedron, by employing the Q_j given in row (a) of table 4. The agreement is perfect because there are more free normal coordinates than available components of $\delta\mathbf{g}$, but the theory presented can only be considered a first approximation. In particular, although the crystal-field theory of point charges gives the right symmetry properties, it is only a very rough description of the physics of the problem.

Although we have not analysed the hyperfine tensor in detail, we have verified that its components are compatible with the normal modes necessary to reproduce the change $\delta\mathbf{g}$ in the **g**-tensor.

3.2. Penta-coordinated Co

3.2.1. The crystal field of the trigonal bipyramid. The structure of the penta-coordinated complex of Co^{2+} is very close to a trigonal bipyramid. Following a method similar to that employed in the octahedral case [15], we chose an orthogonal system of axes X, Y, Z, such that the normal modes obtained from the crystallographic positions would not have contributions from irrelevant rotations and expansions. There are two different Co–O distances in the reference complex: R_a corresponds to the three ligands in the XY-plane (equatorial O) and R_c to the two along the Z-axis (axial O). Two crystal-field parameters D_s and D_t are necessary for the trigonal bipyramid, and can be estimated employing the point charge model [11, 24].

The crystal-field potential V_{CF} can be expressed by the usual formula:

$$V_{CF}(\boldsymbol{r}) = \sum_{kq} \sqrt{\frac{4\pi}{2k+1}} \sum_{\ell} q_\ell \frac{r^k_{\ell<}}{r^{k+1}_{\ell>}} Y^*_{kq}(\theta_\ell, \varphi_\ell) C^{(k)}_q(\theta, \varphi), \tag{3}$$

where $Y_{kq}(\theta_\ell, \varphi_\ell)$ are the spherical harmonics at the position of the ℓth ligand and the $C^{(k)}_q(\theta, \varphi) = \sqrt{4\pi/(2k+1)} Y_{kq}(\theta, \varphi)$ are usually called Racah's rationalized spherical harmonics. In our actual calculation we have employed the real combinations $C_{lm}(\theta, \varphi)$ and $S_{lm}(\theta, \varphi)$ which are proportional to $\cos(m, \varphi)$ and $\sin(m, \varphi)$ respectively [25]. In the absence of the spin–orbit interactions, one employs the irreducible representations Γ of the trigonal bipyramid to classify the eigenstates $|\alpha, S, L, \Gamma, \gamma, a\rangle$ of the Hamiltonian, which are simply related to the states $|\alpha, S, L, M_L\rangle$ (the index α identifies the particular states with the same S, L). In table I of [11] we find that the irreducible representations A'_2, A''_1, A''_2, E', and E'' are contained in the two terms ^4F and ^4P, and that the $|\alpha, S, L, M_L\rangle$ states that generate the corresponding subspaces are $\{|3, 3/2, 3, 0\rangle, |3, 3/2, 1, 0\rangle\} \rightarrow A'_2$, $\{|3, 3/2, 3, \pm 3\rangle\} \rightarrow (A''_1, A''_2)$, $\{|3, 3/2, 3, \pm 2\rangle\} \rightarrow E'$, and $\{|3, 3/2, 3, \pm 1\rangle, |3, 3/2, 1, \pm 1\rangle\} \rightarrow E''$. The Hamiltonian without spin–orbit interaction is diagonal in the partners γ of each irreducible representation Γ and in the spin component M_S, so it is not necessary to write them explicitly here. The only $C^{(k)}_q(\theta, \varphi)$ that contribute to equation (3) in the perfect trigonal bipyramid have $k = 0, 2, 4$ and $q = 0$. To calculate the matrix elements of the Hamiltonian that contains $V_{CF} = \sum_{i=1,7} V_{CF}(\boldsymbol{r}_i)$, we have used the standard tensorial operator techniques [26] as well as the unitary operators obtained from Nielsen and Koster's tables [26,27], and we have verified that our matrix coincides with that given in table 2 of [11].

Our main objective here is to find the gyromagnetic factors that one would expect to measure for the penta-coordinated Co^{2+}, and we shall employ the spectroscopic data measured by means of diffuse reflectance to estimate the parameters B, D_s, and D_t for both $Co{:}Zn_2(OH)PO_4$ and $Co{:}Mg_2(OH)AsO_4$. In the two rows labelled (a) of table 2 we give the corresponding assignments of the transitions from the ground $^4A'_2$ state to the levels with symmetry $^4A''_1$, $^4A''_2$, $^4E''$, $^4E'$, $^4A'_2$(P), and $^4E''$(P), where we use (P) to indicate higher levels of the same symmetry.

From the eigenvalues of the Hamiltonian in the absence of the spin–orbit interaction, we find by trial and error the values of B, D_s, and D_t that minimize the mean square deviation χ for the two systems, and we give them in row (b) of table 5. The transitions calculated with these two sets of values are given in the two rows of table 2 that are labelled (b). The fitting is rather poor, and in particular the transitions to the levels $^4A''_1$, $^4A''_2$, and $^4E''$ fall below the range of the measuring equipment. As an alternative, we have fitted only the three highest transitions, obtaining the values given in row (c) of table 5, and the corresponding values calculated with these two sets of parameters are given in the two rows of table 2 that are labelled (c). In the following section we shall use these two sets of values in order to estimate the gyromagnetic factors for each of the two compounds.

3.2.2. The spin–orbit interaction in the trigonal bipyramid. It is now essential to include the spin–orbit interaction into the calculation. The basis of the irreducible representations Γ_7, Γ_8, and Γ_9 of the double group D^*_{3h} have a simple expression in our system [12]: they are given by $|d^7 \alpha S L J M_J\rangle$, and in particular we have $\Gamma_7(a) \equiv \{|d^7 \alpha S L J \pm 1/2\rangle\}$, $\Gamma_7(b) \equiv \{|d^7 \alpha S L J \pm 11/2\rangle\}$, $\Gamma_8(a) \equiv \{|d^7 \alpha S L J \pm 5/2\rangle\}$, $\Gamma_8(b) \equiv \{|d^7 \alpha S L J \pm 7/2\rangle\}$, $\Gamma_9(a) \equiv \{|d^7 \alpha S L J \pm 3/2\rangle\}$, and $\Gamma_9(b) \equiv \{|d^7 \alpha S L J \pm 9/2\rangle\}$. These states are easily obtained from the $|d^7, \alpha, S, M_S, L, M_L\rangle$ calculated above by employing the 3-j or Clebsch–Gordan coefficients. In the absence of magnetic fields, the two states of each Kramers doublet have the same energy, and to calculate the energies of the system it is enough to consider only the states

Table 5. The values of B, D_s, D_t in cm^{-1} that fit the optical transitions, given in table 2, of the two penta-coordinated complexes. The best fit to the five transitions is given in row (b), and the best fit to the three highest transitions is given in row (c). The spin–orbit parameter $\zeta = 580\ cm^{-1}$ was used in all these fittings.

	PO_4			AsO_4		
	B	D_s	D_t	B	D_s	D_t
(b)	728	165	947	785	313	919
(c)	852	745	885	875	749	869

with positive M_J. As only the mixture of the ^4F and ^4P states is important in our problem, we shall consider only that subspace, and the corresponding matrix of the total Hamiltonian splits into five boxes of the following dimensions: $(M_J = 1/2) \rightarrow \Gamma_7(a) \rightarrow (7\times7)$, $(M_J = 3/2) \rightarrow \Gamma_9(a) \rightarrow (6 \times 6)$, $(M_J = 5/2) \rightarrow \Gamma_8(a) \rightarrow (4 \times 4)$, $(M_J = 7/2) \rightarrow \Gamma_8(b) \rightarrow (2 \times 2)$, $(M_J = 9/2) \rightarrow \Gamma_9(b) \rightarrow (1 \times 1)$, and there are no matrix elements for $M_J = 11/2$, i.e. $\Gamma_7(b)$, within the subspace $\{^4F, ^4P\}$ of d^7 that corresponds to $S = 3/2$. The matrices that we have obtained coincide with those given in table 2 of [12], and their eigenvalues have been calculated for the different sets of B-, D_s-, and D_t-values that were obtained above, employing the one-electron spin–orbit parameter $\zeta = 580\ cm^{-1}$. For all the set of parameters in table 5 the lowest doublet is $\Gamma_7(a)$ $(M_J = \pm1/2)$, separated by at least 75 cm^{-1} from the following $\Gamma_9(a)$ $(M_J = 3/2)$ doublet, and by more than 2377 cm^{-1} from the remaining doublets. This situation is not altered by making fairly large changes in the three basic parameters B, D_s, and D_t, and this shows that even for moderate increases in the temperature only the lowest doublet $(M_J = \pm1/2)$ would be occupied. This doublet has allowed ESR transitions, and they should be observed within the approximation employed. If the positions of the two lowest doublets were exchanged, the ESR transitions of the lowest doublet would be forbidden and the spectra should not then be observed.

The fact that the two lowest doublets have $M_J = \pm1/2$ and $M_J = \pm3/2$ and are separated by a large energy from the remaining doublets is easily understood when we notice that the lowest level in the absence of spin–orbit interaction is $^4A_2'$. The orbital part A_2' is a singlet with no orbital angular momentum, and the total $\boldsymbol{J}$ would then correspond to $S = 3/2$. These four states would be rather far apart from the remaining ones, and would split in the way calculated above through the higher-order spin–orbit mixing with those excited states.

The present calculation was for a perfect trigonal bipyramid with D_{3h} symmetry, and one might wonder whether deformations with respect to this structure could alter the relative positions of the two lowest doublets, thus causing a change from an allowed to a forbidden ESR transition. We shall hence study the effect of these deformations, both on the relative positions of the two lowest doublets and on the value of the gyromagnetic tensor. In this study we shall follow a treatment similar to that employed in the octahedral case, by considering the effect of the normal modes of the trigonal bipyramid on the Hamiltonian of the penta-coordinated Co^{2+}.

3.2.3. The normal modes of the trigonal bipyramid. As in the octahedral case, we are interested in a contribution to the Hamiltonian of the same type as equation (1), but here the normal modes Q_j and $V_j(\boldsymbol{r})$ transform like the same partners of irreducible representations of the trigonal bipyramid. As the undistorted complex does not have a centre of symmetry, both the even and odd modes, under reflection in the equatorial plane, may have non-zero matrix elements within the configuration d^7 of Co^{2+}, and therefore we shall need to consider both types of normal mode in our discussion.

The departures of the six atoms of the complex span a reducible representation Γ of the D_{3h} group, that can be reduced as follows: $\Gamma = 2A_1' + A_2' + 4E' + 3A_2'' + 2E''$ (see e.g. equation (9.19) in [28]). Of these irreducible representations, A_2' corresponds to an axial rotation, one E'' to two equatorial rotations, one A_2'' to an axial translation, and one E' to two equatorial translations. After eliminating these three translations and rotations, we are left with three even irreducible representations E', as well as two A_2'' and one E'' odd representations. The six even normal modes ($Q_1, \ldots, Q_6$) transform in pairs like the partners of E', and together with the two modes A_2'' (Q_7, Q_8) and the two partners of E'' (Q_9, Q_{10}) have been obtained employing standard techniques [15, 28, 29].

The modes Q_3, Q_4, and Q_8 are translations of only the two axial oxygens, and the Q_5, Q_6, and Q_7 are translations of only the three equatorial oxygens, while Q_9 and Q_{10} are rotations around the x- and y-axes of the two axial oxygens. As these modes are only partial rotations or translations, they are capable of changing the crystal field. The x- and y-rotations of the three equatorial oxygens can be combined with Q_9 and Q_{10} to give full rotations of the trigonal bipyramid, and the z-rotation of the three equatorial oxygens is already a full rotation, so these three sets of displacements would not appear in our calculation.

3.2.4. The effect of the normal modes on the crystal field. By expansion of equation (3) we have obtained an expression similar to equation (1) for the trigonal bipyramid [15]. As we are only interested in the subspace $\{^4F, ^4P\}$ with $S = 3/2$ of the configuration d^7, and the $V_j(\boldsymbol{r})$ are independent of the spin component M_S, we need a 10×10 matrix $\langle {}^4L, M_S, M_L | V'_{CF} | {}^4L', M_S, M'_L \rangle$ for each Q_j, with fixed M_S and $L, L' = 3, 1$. It is interesting to note that the matrix elements associated with Q_3, Q_4, and Q_8 are all zero: these modes involve only the two axial ions, and the corresponding two-atom partial complex is not only invariant under the operations of D_{3h}, but also under rotation about a twofold axis along the z-direction. This extra symmetry forces all the one-electron matrix elements connecting d states of the crystal field associated with Q_3, Q_4, and Q_8 to be zero.

The crystal field V'_{CF} generated by the relevant normal mode Q_j has coefficients containing the Co–O distances R_a and R_c, as well as the atomic averages $\langle r^2 \rangle$ and $\langle r^4 \rangle$. As R_a and R_c are nearly the same, it is possible to express V'_{CF} employing instead the crystal-field parameters D_s and D_t [15].

As with the reference complex, we employ the 3-j coefficients to calculate the matrix elements of the crystal field V'_{CF} in the representation that diagonalizes the total J and J_z, because the doublets $|d^7 \alpha S L J M_J \rangle$ are the basis for the irreducible representations of the reference trigonal bipyramid, and the eigenstates of the reference complex would then belong to subspaces with fixed M_J. In section 3.2.2 we have shown that, with the two sets of parameters B, D_s, and D_t obtained in that section, the two lowest doublets belong to the $M_J = 1/2$ and $M_J = 3/2$ subspaces and that they are separated by more than 75 cm^{-1}, while the remaining doublets are more than 2300 cm^{-1} above them. A good approximation to use for calculating the effect of V'_{CF} on these levels is then to consider the total Hamiltonian inside the two subspaces $M_J = 1/2, 3/2$, and one has then to consider a matrix of 26×26 elements, corresponding to values of J equal to $9/2, \ldots, 1/2$. The eigenstates of this matrix show that there is no change in the relative positions of the two lowest doublets, so the ground-state remains $M_J = 1/2$, still leaving open the origin of the low intensity of the ESR spectrum of the penta-coordinated complex.

3.2.5. The g-factors of the penta-coordinated Co^{2+}. To calculate the spin Hamiltonian we employ the traditional method [23]. In the present case we consider the four states of the two lowest doublets of the reference trigonal bipyramid calculated in section 3.2.2 as the eigenstates

Table 6. The principal components of the calculated **g**-tensor for penta-coordinated Co^{2+} and their average g_{av} for $Co{:}Zn_2(OH)PO_4$ and $Co{:}Mg_2(OH)AsO_4$. Rows (b_0) and (c_0) are for the reference trigonal bipyramid, while rows (b_1), (b_2), (b_3), (c_1), (c_2), and (c_3) include the effect of deformations produced by the crystallographically calculated normal modes (see the text).

	g_1	g_2	g_3	g_{av}
PO_4				
(b_0)	4.8027	4.8027	1.9904	3.8653
(b_1)	5.0477	4.5577	2.2998	3.9684
(b_2)	5.0477	4.5577	1.9904	3.8653
(c_0)	5.0435	5.0435	1.9829	4.0233
(c_1)	5.7379	4.3492	2.1171	4.0680
(c_2)	5.7379	4.3492	1.9829	4.0233
AsO_4				
(b_0)	4.8723	4.8723	1.9885	3.9110
(b_1)	5.7637	4.2279	2.2364	4.0760
(b_2)	5.7637	4.2279	1.9885	3.9934
(b_3)	5.6402	4.1044	1.9885	3.9110
(c_0)	5.0667	5.0667	1.9818	4.0384
(c_1)	7.1232	3.5385	1.9854	4.2157
(c_2)	7.1232	3.5385	1.9818	4.2145
(c_3)	6.8591	3.2744	1.9818	4.0384

of the unperturbed Hamiltonian, with $M_J = 1/2$ as the ground doublet and $M_J = 3/2$ as the excited one. Both the Zeeman term and the crystal field V'_{CF} produced by the deformation of the normal modes are perturbations, and in the usual way we find the gyromagnetic tensor **g** in second order. We have calculated the three components of **g** for the penta-coordinated Co^{2+} for all the sets of B, D_s, and D_t given in table 5, and the results are given in table 6. The values corresponding to the reference trigonal bipyramid are given in the rows (b_0) and (c_0), while those given in the rows (b_j) and (c_j) (with $j = 1, 2$ for the phosphate and $j = 1, 2, 3$ for the arsenate) have been calculated employing the normal modes Q_j derived from the crystallographic positions as discussed in section 3.2.3. It is verified in table 6 that the average of the principal values of g is not very different from 4.33, but that it changes with B and the crystal-field parameters more than in the octahedral case. The rows (b_1) and (c_1) include the effects of all normal modes, while in rows (b_2) and (c_2) only the even modes are considered. In the phosphate case, the crystallographic $Q_1 = Q_5 = 0$, and for the arsenate we have also imposed this condition in rows (b_3) and (c_3).

From the calculations in the present section, it follows that one should observe an allowed ESR line of Co^{2+} from the penta-coordinated complex when that site is occupied. We have seen in section 2.3 that, besides the lines associated to the octahedral spectra, there are some weak extra lines that could be interpreted as belonging to that complex: their estimated g-factors are given in rows (b) of table 3, and should be compared with the values given in table 6, that were calculated for different sets of parameters derived from the optical spectra and with normal modes calculated from the crystallographic positions. It is clear that the arsenate values in row (c_3) of table 6 are fairly close to the estimated values in row (b) from table 3. It is well known that the g_i obtained from the crystallographically calculated normal modes are generally different from those observed experimentally, as discussed for the octahedral compounds (cf section 3.1), and we could anticipate that a good fitting could be obtained by making small changes in the crystallographic normal modes. To verify this assumption it is sufficient to

change only Q_2 and Q_6, keeping all the remaining modes at their crystallographic values. Employing $Q_2/R_a = -0.03$ and $Q_6/R_a = -0.07$ for the phosphate, we find $g_1 = 7.05$, $g_2 = 3.03$, and $g_3 = 2.12$, while for the arsenate we obtain $g_1 = 7.62$, $g_2 = 3.04$, and $g_3 = 1.99$ with $Q_2/R_a = 0.01$ and $Q_6/R_a = -0.07$. These fittings are fairly good, and show that the ESR spectra of Co^{2+} in the two compounds can be described perfectly well within our theory, but one should not place too much reliance on the crystal fields obtained because of the very large errors in the experimental **g**-tensor.

We notice that the relative intensities of the extra lines in figure 2 are rather smaller than those in figure 3. This can be understood because the concentration of Co^{2+} in the arsenate is ten times larger than in the phosphate, and this should also alter their relative occupations.

The rather low intensity of the lines that could be attributed to the penta-coordinated complex indicates a very low occupation of Co^{2+} in the penta-coordinated sites. To verify this conjecture, we present a molecular orbital calculation of the heat of formation of these compounds in the following section, and the results are compatible with the present conclusion.

3.3. Molecular orbital calculations

The energetics of penta- and hexa-coordinated phosphate clusters has been assessed in terms of molecular orbital theory. Heats of formation were calculated within the well known semi-empirical technique 'Parametric Model 3' (PM3) [30]. This is a technique derived from the Hartree–Fock approximation in combination with a minimal-basis-set expansion of the molecular orbitals. Here we used a special parametrization developed for transition metal atoms which is contained in the package SPARTAN [31]. Correlation and relativistic effects, which are not explicitly treated in this theory, are partly recovered from the adopting of experimental data in the parametrization. The molecular geometries were obtained as follows. The central metal atom and the coordinates of the first neighbouring five or six oxygen atoms were taken from the crystal structure of the compound $Co_2(OH)PO_4$. The ligands were chosen to be phosphoric acid molecules, $OP(OH)_3$, since they have all bonds saturated and are neutral. Geometry optimizations of the isolated ligand were carried out at the *ab initio* 6–31G** level of calculation, in which each atomic orbital of the basis set is written as a linear combination of Cartesian–Gaussian functions [32]. The proton-free oxygen atoms of the ligands were then placed in the crystallographic positions of the oxygens around the metal atom such that the O = P bond points in the M–O direction, as shown in figures 4 and 5. The PM3 heats of formation of the clusters $[M(OP(OH)_3)_n]^{2+}$, $n = 5, 6$ and M = Co and Zn, were calculated assuming that Zn ion just replaces the Co ion at frozen ligand positions. This is a reasonable assumption since the pure Co and Zn crystals have very similar cell parameters. Co clusters are doublets, so the unrestricted (spin-polarized) PM3 Hamiltonian was adopted. Spin contamination was negligible in this calculation. In order to allow us to discount the energies associated with the ligands themselves, the heats of formation of the corresponding clusters without the central metal ion were computed. Results are shown in table 7. The values in the first column are the contributions from the ligands to the metal cluster heats of formation. It is then possible to evaluate the relative stabilization of Co^{2+} and Zn^{2+} ions in the penta- and hexa-coordinated environments by taking the difference between the values in columns two or three and column one. This gives the energies -1258.04 and -1314.30 kcal mol^{-1} for Co^{2+} at the trigonal bipyramidal and octahedral sites, respectively, while for Zn^{2+} the values are 346.19 and 340.00 kcal mol^{-1}. These values show that Co has a preference for the octahedral site amounting to $\sim$56 kcal, which is approximately 2.4 eV, and Zn is also slightly more stable at the octahedral site, by $\sim$6 kcal, or 0.3 eV. This difference is due to the partially filled 3d orbitals of Co that interact with the lone pairs of the neighbouring oxygens, imparting a more covalent character to the interaction.

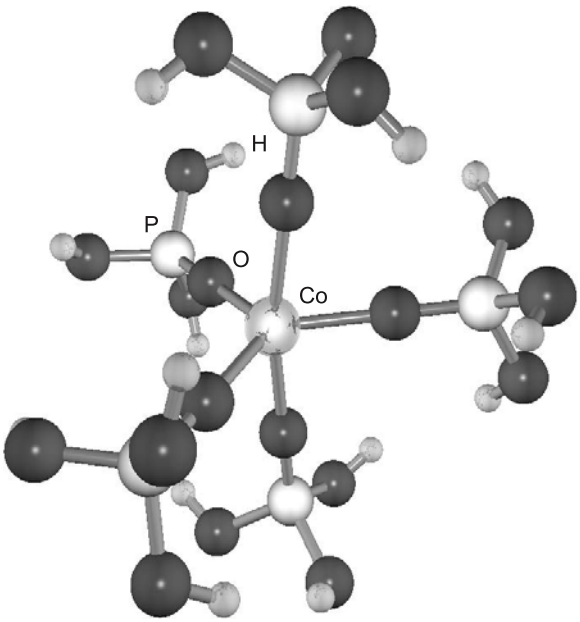

Figure 4. A ball-and-stick model of the penta-coordinated metal clusters with phosphoric acid molecules as ligands. One atom of each type is labelled in the figure.

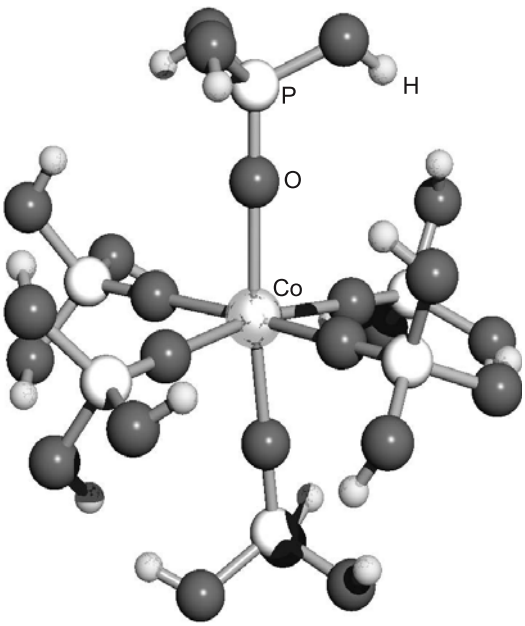

Figure 5. A hexa-coordinated metal/phosphoric acid cluster. One atom of each type is labelled in the figure.

A more direct comparison was made through the calculation of the heat of formation for clusters where the metal atoms and first neighbours are in the conformation of the $Co_2(OH)PO_4$ unit cell, as illustrated in figure 6. Two clusters were built such that in one the Co^{2+} ion occupies the hexa-coordinated site and the Zn^{2+} ion is in the penta-coordinated

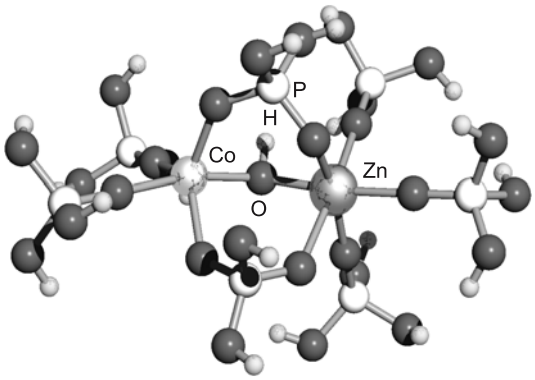

Figure 6. The cobalt/zinc cluster built from the atomic coordinates of the $Co_2(OH)PO_4$ unit cell. Some of the phosphate ions were replaced by phosphoric acid molecules. One atom of each type is labelled in the figure, which shows the Co in the penta-coordinated position.

Table 7. Heats of formation, in kcal mol^{-1}, from PM3 calculations.

ΔH_f (kcal mol^{-1})	No ion	Co^{2+}	Zn^{2+}
$[M(OP(OH)_3)_5]^{2+}$	−1214.69	−2472.73	−868.50
$[M(OP(OH)_3)_6]^{2+}$	−1440.16	−2754.45	−1100.15

site (cluster 1), while in the other (cluster 2), the Co^{2+} and Zn^{2+} ions are exchanged. The phosphate ions in contact with both metal ions were replaced by H_2PO_4 species and the remainder of the ligands were phosphoric acid molecules. The composition of these clusters is then $[CoZn(OH)(H_2PO_4)_2(OP(OH)_3)_5]^{4+}$. PM3 calculations gave ΔH_f(cluster 1) = −2147.10 kcal mol^{-1} and ΔH_f(cluster 2) = −2094.44 kcal mol^{-1}; that is, the cluster with Co^{2+} ion in the octahedral site is ∼53 kcal more stable than the other one. One thus expects Co impurities in the zinc compounds to occupy preferentially the octahedral sites, and this conclusion agrees with the very low intensity of the ESR lines attributed to Co^{2+} in the penta-coordinated sites of the dilute compounds, as discussed in the previous section.

4. Discussion and conclusions

Four compounds of the adamite type: $Zn_2(OH)PO_4$, $Mg_2(OH)AsO_4$, $Co_2(OH)PO_4$, and $Co_2(OH)AsO_4$, have been synthesized and studied, and the measurements of the optical properties of the pure Co compounds and of the ESR of impurities of Co^{2+} in $Zn_2(OH)PO_4$ and $Mg_2(OH)AsO_4$ have been discussed. Crystal-field theory has been employed in an attempt to understand the experimental ESR results for the two Co^{2+} complexes with coordination five and six that are present in the adamite structure. The Racah parameter B as well as the crystal fields Dq for the octahedral complex and both D_s and D_t for the trigonal bipyramidal one have been estimated from the assignments that were made of the diffuse reflectance spectrum for these two complexes. Two alternative sets of parameters were proposed for the penta-coordinated complex.

From the crystallographic structure, a reference octahedron centred on the Co^{2+} was defined, such that the normal modes of the complex corresponding to rotations and expansions would be zero and the remaining normal modes would not contain any contribution from these irrelevant deformations. Using a method already applied [10] to study the ESR of Co^{2+} in $NH_4NiPO_4{\cdot}6H_2O$, the crystal fields that would reproduce the experimental **g**-tensor of the octahedral complex in both $Zn_2(OH)PO_4$ and $Mg_2(OH)AsO_4$ have been obtained.

As the penta-coordinated complex seems to make at most minor contributions to the ESR spectra, we have analysed the possible reasons for this behaviour. We argue that two doublets with $M_J = \pm 1/2$ and $M_J = \pm 3/2$ would be lowest in energy, separated by a rather large excitation energy from the remaining excited states. The $M_J = \pm 3/2$ doublet has forbidden ESR transitions, and this would explain the experimental results if that were the ground doublet, but when the crystal field of the trigonal bipyramid is considered together with the spin–orbit interaction, it was found that the $M_J = \pm 1/2$ doublet, with allowed ESR transitions, is the lowest. To verify whether this result would be altered by the deformations of the trigonal bipyramid, we considered their effects in a way similar to that employed in the octahedral case to calculate the **g**-tensor. It was necessary to derive the normal modes of the trigonal bipyramid that are relevant to our problem, as well as the corresponding Jahn–Teller contributions V'_{CF} to the crystal field [15]. Defining a reference perfect trigonal bipyramid by the same method as was employed in the octahedral case, the values of the relevant normal modes were obtained by employing the crystallographic positions, and subsequently used to calculate their effect on the relative position of the two lowest doublets. No appreciable change was found, and as an alternative explanation we assumed that the penta-coordinated complex is scarcely occupied in the dilute system. To verify this conclusion, the heats of formation of the octahedral and the trigonal bipyramidal complexes with Co and with Zn as the central ions were calculated, and it was found that their values are compatible with a rather low occupation of the penta-coordinated site.

Employing the Jahn–Teller crystal fields together with the normal modes calculated from the crystallographic distortions, it was possible to calculate the **g**-tensor, shown in table 6, for both the perfect and the deformed trigonal bipyramid, this latter subjected to different deformations. The trace of the **g**-tensor in the perfect trigonal bipyramid changes more with the parameters B, D_s, and D_t than in the octahedral case, where it is always fairly close to 13.

The trigonal bipyramid has no centre of symmetry, and it was necessary to consider all the normal modes, even those that are odd under reflection in the horizontal symmetry plane. We have shown that these latter modes affect the axial component of **g** but that they have little or no effect on the two equatorial components. The experimental **g**-tensor of the penta-coordinated complex could be measured, but with rather large errors. As in the octahedral case, the crystallographically determined normal modes could not explain the observed values, but for the two types of complex it was possible to find the crystal fields that reproduce the experimental ESR spectra for both the phosphate and arsenate compounds.

We conclude that our theoretical analysis of the ESR of the systems studied and the molecular orbital calculation of the formation energies coincide in assigning a rather low relative occupation of the penta-coordinated sites with respect to the octahedral ones in these systems. We were also able to explain the experimental ESR spectra of the octahedral and of the penta-coordinated complexes by considering the effect of the crystal fields on the **g**-tensor.

Acknowledgments

The three first authors (MEF, MCS, GEB) would like to acknowledge financial support from the following agencies: FAPESP and CNPq.

References

[1] Riffel H, Zettler F and Hess H 1975 *Neues Jahrb. Mineral. Monatsh.* 514
[2] Richmond W E 1940 *Am. Mineral.* **25** 441
[3] Hawthorne F C 1976 *Can. Mineral.* **14** 143
[4] Hill R J 1976 *Am. Mineral.* **61** 979

[5] Harrison W T A, Vaughey J T, Dussack L L, Jacobson A J, Martin T E and Stucky G D 1995 *J. Solid State Chem.* **114** 151
[6] Keller P 1971 *Neues Jahrb. Mineral. Monatsh.* 560
[7] Keller P, Hess H and Zettler F 1979 *Neues Jahrb. Mineral. Abh.* **134** 147
[8] Rojo J M 2000 *PhD Thesis* Universidad del Pais Vasco, Bilbao
[9] Abragam A and Bleaney B 1970 *Electron Paramagnetic Resonance of Transition Ions* (Oxford: Clarendon) p 449
[10] Goñi A, Lezama L M, Rojo T, Foglio M E, Valdivia J A and Barberis G E 1998 *Phys. Rev.* B **57** 246
[11] Beltran F G and Palacio F 1976 *J. Phys. Chem.* **80** 1373
[12] Palacio F 1978 *J. Phys. Chem.* **82** 825
[13] Jahn H A and Teller E 1937 *Proc. R. Soc.* A **161** 220
[14] Jahn H A 1937 *Proc. R. Soc.* A **164** 117
[15] In the present work it was necessary to derive many properties of the normal modes and crystal fields of the two complexes, and a detailed description of the procedures and necessary tables can be found in:
Foglio M E, dos Santos M C, Barberis G E, Rojo J M, Mesa J L, Lezama L and Rojo T 2001 *Preprint* cond-mat/0110563
in the LANL e-print archives. Most of these tables and details have been omitted from the present paper for brevity.
[16] Rojo J M, Mesa J L, Lezama L, Barberis G E and Rojo T 1996 *J. Magn. Magn. Mater.* **157+158** 493
[17] Rojo T, Lezama L, Rojo J M, Insausti M, Arriortua M I and Villeneuve G 1992 *Eur. J. Solid State Inorg. Chem.* **29** 217
[18] Rojo M M, Mesa J L, Pizarro J L, Lezama L, Arriortua M I and Rojo T 1997 *J. Solid State Chem.* **132** 107
[19] Van Vleck J H 1939 *J. Chem. Phys.* **7** 72
[20] Koster G F, Dimmock J O, Wheeler R G and Stats H 1963 *Properties of the Thirty-Two Point Groups* (Cambridge, MA: MIT Press)
[21] Tinkham M 1956 *Proc. R. Soc.* A **236** 549
[22] Abragam A and Pryce M H L 1951 *Proc. R. Soc.* A **206** 173
[23] Pryce H M L 1950 *Proc. R. Soc.* A **63** 25
[24] Wood J S 1968 *Inorg. Chem.* **7** 852
[25] Griffith J S 1961 *The Theory of Transition-Metal Ions* (Cambridge: Cambridge University Press) equation (6.37)
[26] Fano U and Racah G 1959 *Irreducible Tensorial Sets* (New York: Academic)
[27] Nielsen C W and Koster G F 1963 *Spectroscopic Coefficients for the p^n, d^n and f^n Configurations* (Boston, MA: MIT Press)
[28] Woodward L A 1972 *Introduction to the Theory of Molecular Vibrations and Vibration Spectroscopy* (Oxford: Clarendon)
[29] Wilson E B, Decius J C and Cross P C 1955 *Molecular Vibrations* (New York: McGraw-Hill)
[30] Stewart J J P 1989 *J. Comput. Chem* **10** 209
[31] *SPARTAN Package* 1995 version 5 (Wavefunction Incorporated)
[32] For basis set definitions, see for instance
Szabo A and Ostlund N S 1989 *Modern Quantum Chemistry* (New York: McGraw-Hill)